

1 Energy and economic analysis feasibility of CO₂ capture on a natural gas internal 2 combustion engine

3 Alexander García-Mariaca^{1*} and Eva Llera-Sastresa²

4 ^{1*} Escuela de Ingeniería y Arquitectura, University of Zaragoza, María de Luna s/n, Zaragoza,
5 50018, Spain; alexander.garcia@unizar.es

6 ² Department of Mechanical Engineering and CIRCE Research Institute, University of Zaragoza,
7 María de Luna s/n, Zaragoza, 50018, Spain; ellera@unizar.es

8 9 Abstract

10 CO₂ capture by amine scrubbing is a widely developed technology in its most advanced stage of
11 evolution. However, it has never been used to capture CO₂ from mobile sources. The present study
12 performs a thermo-economic analysis of an amine scrubbing CO₂ capture storage (CCS) system,
13 which takes for the amine regeneration process the waste heat from the exhaust gases of a
14 turbocharged natural gas internal combustion engine (mobile source). The selected engine for the
15 study is an M936G, widely used in freight and passenger transport. A primary and a tertiary amine
16 were chosen for the simulations. In order to reduce volume and increase autonomy, captured CO₂
17 is stored as a liquid; therefore, a specific installation is planned. The system is hybridised with an
18 Organic Rankine Cycle (ORC) to reduce the energy penalty on the CCS system. Results show that
19 a CCS system operating with Monoethanolamine (MEA) at 30 wt% achieved a maximum CO₂
20 capture rate of 66%, with a penalty over the power engine of only 10%. On the other hand, the
21 economic analysis showed that the CCS system with MEA and without ORC is 31.8% cheaper
22 than a hydrogen fuel cells bus and 26% cheaper than a battery-electric bus.

23 Keywords: CO₂ capture. Amine-scrubbing, internal combustion engines, Organic Rankine Cycle.

24 1. Introduction

25 Currently, the transport sector contributes 25% of total CO₂ emissions and is gradually migrating
26 towards electrification to reduce its CO₂ footprint¹. However, in freight and passenger transport,
27 battery electric vehicles (BEV) and fuel cell vehicles (FCV) can only be a supplement, but not an
28 alternative, to classic combustion engines², due to short autonomies. This sector is expected to
29 continue operating with C-H chain fuels, and the challenge focuses on fuels such as natural gas or
30 synthetic natural gas. If, as in this last case, CH₄ is elaborated with a CO₂ captured (in an onboard

31 Internal combustion engine vehicle) as raw material and an energy surplus from renewable
32 sources, it could close the gap and drive the transport sector towards zero CO₂ emissions.

33 CCS is a potential technology for reducing CO₂ emissions and sustainable energy production^{3,4}.
34 The CCS systems allow CO₂ to be separated from a gas stream before or after a combustion
35 process⁵. These technologies have mainly been applied in the heat and power generation sector
36 and industries, such as cement and steel production⁶. In particular, CO₂ capture technologies in
37 post-combustion have had significant advances in recent years. Whereby the use of these
38 technologies in the transport sector could be functional. Some authors suggest that amine
39 scrubbing, adsorption, and membranes could be adapted to operate on mobile sources^{7,8}.

40 So far, the research about CCS systems in mobile sources has been focused on absorption and
41 adsorption. Engine-driven ships are the most favourable scenario for an absorption installation
42 because the internal combustion engine (ICE) operates almost at the same load condition in a
43 journey, which is quite like the operating conditions of a power plant. Ship-based carbon capture
44 (SBCC) research works have focused on amine scrubbing facilities. They have made economic
45 analyses and evaluated several amines in different proportions, CO₂ capture rates (CCR), and the
46 use of waste energy recovery systems.

47 For instance, Awoyomi et al.⁹ studied the effect of exhaust gas recirculation (EGR) on an LNG-
48 fuelled ship. They obtained a CCR of 90% with a solvent of NH₃ in a concentration of 4 wt% and
49 solvent flow close to 40 kg/s. Stec et al.¹⁰ evaluated in a diesel-fuelled ship an amine-scrubbing
50 facility under three atmospheric conditions (arctic, ISO, and tropical) using a solvent with
51 Monoethanolamine (MEA) at 30 wt%. The best results were found under tropical conditions with
52 values of CCR of 91.4%, 2.249 MW of heat duty, and a regeneration heat of 3.61 MJ/kgCO₂.
53 Güler and Ergin¹¹, in several LNG-fuelled ships, evaluated an amine-scrubbing facility with a
54 solvent concentration of 35 wt% of MEA. The average result of CCR obtained in their study was
55 33%. Ros et al.¹² evaluated SBCC on 12 LNG-fuelled engines (8 MW each) with a solvent of 30
56 wt% of MEA. The main results were a maximum CCR of 81% with an average price of 125
57 €/CO₂ton (depending on the storage pressure of CO₂). Luo and Wang¹³, in a diesel-fuelled ship of
58 10.8 MW with a waste energy recovery system (WERS), made an economic analysis of an amine-
59 scrubbing plant using MEA at 30 wt% as solvent. The results show a CCR of 73% and a CO₂
60 capture price of 77.5 €/CO₂ton without the WERS. With WERS, 90% of CCR is reached with a

61 higher CO₂ capture price of 163 €/CO₂ton. Feenstra et al.¹⁴ evaluated two solvents, MEA and
62 piperazine (PZ), for the CO₂ capture process on a 3 MW LNG-fuelled ship. The main conclusion
63 of their study is that the cost of CO₂ capture is 120 €/CO₂ton using MEA and 98 €/CO₂ton using
64 PZ.

65 In contrast, in ICE vehicles (ICEv), their rapid accelerations and decelerations and changes in the
66 speed and load in the engine are the bottlenecks that do not allow the implementation of CCS
67 systems in this sector. The research works found in the literature have evaluated the energy
68 requirements of the CCS system and the kind most suitable sorbent or solvent. Sharma and
69 Maréchal¹⁵ elaborated an energy analysis of a CCS system by temperature swing adsorption (TSA)
70 on a diesel-fuelled engine of a truck. The main result obtained is that with a WERS taking the
71 thermal energy exhaust gases in advantage and with PPN-6-CH₂-TETA as sorbent, the CCS
72 system does not have penalisation over the ICE with a CCR of 90%. García and Llera⁵ presented
73 an energy analysis of a CCS system with TSA operating with several sorbents. The CCS system
74 is hybridised with an organic Rankine cycle (ORC) to supply the utilities of the CCS system. The
75 main conclusion obtained is a 73% of CCR with MOF-74-Mg without penalisation over the engine.

76 Regarding absorption, Kumar et al.^{16,17} evaluated MEA, methyl diethanolamine (MDEA) and
77 blends with NH₃ on a diesel-fuelled engine. The main result of these investigations is that MEA
78 has a CO₂ reduction overcome 90% in any engine load condition. However, these research works
79 do not show as is the CO₂ capture unit and the operating parameters of this.

80 As shown above, CO₂ capture by absorption in ICEv has a few scientific developments, and this
81 study aims to broaden the knowledge of this field. This research paper presents the first thermo-
82 economic study of a CCS system onboard a natural gas (NG) fuelled vehicle operating in the entire
83 rpm operating range and under four engine load conditions. The CCS system proposed is subject
84 to a sensitivity analysis using a primary and tertiary amine with 30 wt% in the solvent. Evaluations
85 are carried out also with the hybridisation of an ORC that takes the exhaust gases' thermal energy
86 to supply the amine-scrubbing and CO₂ compression utilities. The simulation of the different
87 processes was carried out in Aspen Plus. The feasibility analysis aims at answering the following
88 questions: i) Is the intended heat integration of the exhaust gases with the CCS systems and ORC
89 thermally feasible? ii) What is the maximum CCR with the primary and tertiary amines? iii) How

90 much is the purchase cost of a vehicle with a CCS system installed? vi) What is the power
91 penalisation of the CCS over the engine performance?

92 **2. Methodology**

93 The energy analysis of CO₂ capture on board an ICEv through amine scrubbing developed in this
94 research involves integrating three systems: the ICE (CO₂ generator), the CCS system, and the
95 WERS. Ideally, the thermal energy required for CO₂ desorption should come from the exhaust
96 gases of the vehicle's engine, and the electricity for the operation of the CCS system devices should
97 come from the engine and from the WERS, which in the case of this study will be an organic
98 Rankine cycle (ORC). After technical analysis, an economic analysis is performed. The evaluated
99 total capital expenditure (CAPEX) will be used to establish whether the hybridisation of these
100 three systems in an ICEv for CO₂ reduction is competitive with other CO₂ reduction technologies
101 available in the market. Each component and procedure developed in the simulations are described
102 below.

103 **2.1.Engine selection and model**

104 2.1.1. Engine selection

105 In the short and medium term, ICEvs will keep using carbon-based fuels while the transport sector
106 migrates completely towards electrification. Gaseous fuels such as natural gas (mainly CH₄) will
107 be one of the best choices because of the high lower heating value (LHV) and short carbon chain
108 that produces less CO₂^{18, 19}. Under this basis, a heavy-duty turbocharged natural gas (NG) spark
109 ignition (SI) engine of reference M936G has been selected to run the simulations. This engine is
110 widely used in trucks and buses. The technical specifications of the engine are summarised in
111 Table 1.

112 Table 1. Technical specifications of the M936G engine²⁰.

Architecture	In-line 6-cylinder engine
Aspiration method	Turbocharged with Aftercooler
Injection	Multipoint
Valves per cylinder:	4
Bore [mm]	110
Stroke [mm]	135
Displacement volume [cm ³]	7700
Compression ratio	17
Brake Power [kW]	222 at 1950 rpm
Torque [Nm]	1200 at 1600 rpm

113 2.1.2. Engine simulation

114 The selected SI-ICE is simulated over AVL BOOST software to determine the pressure,
 115 temperature, and concentration of the engine exhaust gases at the catalytic converter outlet. The
 116 simulations were performed at four engine load conditions (25, 50, 75 and 100%) in the rotational
 117 speed range of 1000 to 1900 rpm. The models used in the simulations are the Heywood, Patton,
 118 and Nitschke model for the friction, the Woschni heat transfer model for the heat transfer in the
 119 cylinders, and the Re-analogy for the heat transfer in the engine ducts. Finally, the air inlet is at
 120 standard conditions. The main input parameters to run the simulations are listed in Table 2.

121 Table 2. Input parameters in AVL BOOST for the engine simulations

Variable	Unit	M936G
Firing Order	NA	1,5,3,6,2,4
Star of combustion	CAD	-18
Combustion duration	CAD	57
A/F ratio	-	Stoichiometric combustion [16.75]
Maximum boost pressure ratio	-	2
Connecting Rod Length	mm	250
Lower heating value NG ^{21, 22, 23}	MJ/kg	48351

122 2.1.3. Engine Model validation

123 The results of brake power (BP) and brake-specific fuel consumption (BSFC) obtained in the
 124 simulations are validated with the values given by the manufacturer for these variables²⁰. As can
 125 be seen in Table 3, the maximum error between the simulation and the manufacturer values is
 126 6,63%. Therefore, the results obtained in the engine simulation present an appropriate behaviour,
 127 considering that the pressure, temperature, concentration, and exhaust gases mass flow are close
 128 to reality.

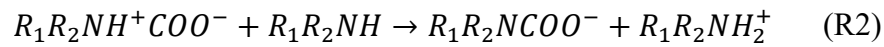
129 Table 3. Comparison engine results between the simulation and manufacturer chart

Engine load [%]	rpm	Real ²⁰		Simulation		Error	
		BP [kW]	BSFC [g/kWh]	BP [kW]	BSFC [g/kWh]	BP [%]	BSFC [%]
100%	1000	110,0	200,00	110,17	192,04	-0,2%	4,0%
	1400	181,0	186,00	174,98	187,81	3,3%	-1,0%
	1600	204,0	188,00	197,27	188,33	3,3%	-0,2%
	1900	220,0	193,00	227,45	189,60	-3,39%	1,76%
75%	1000	82,5	225,00	82,91	221,52	-0,50%	1,54%
	1400	135,75	209,25	136	209,19	-0,18%	0,03%
	1600	153	211,50	153,6	211,57	-0,39%	-0,03%
50%	1000	55	270,00	55,26	269,47	-0,47%	0,19%
	1400	90,5	251,10	96,5	246,57	-6,63%	1,80%
	1600	102	253,80	104,36	253,61	-2,31%	0,07%
	1900	110	260,55	112,45	260,77	-2,23%	-0,09%
25%	1000	27,5	416,00	27,42	421,00	0,29%	-1,20%
	1400	45,25	386,88	45,26	387,11	-0,02%	-0,06%
	1600	51	391,04	50,69	391,21	0,61%	-0,04%
	1900	55	401,44	54,01	401,36	1,80%	0,02%

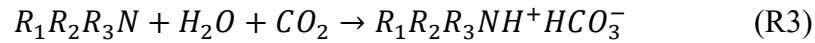
130 **2.2. Model development of the amine-scrubbing and CO₂ compression facilities**

131 2.2.1. Amine selection

132 Amines are organic compounds used for CO₂ capture since the 1930s becoming an effective
 133 method widely used in the industry for this purpose²⁴. They are usually diluted in water in
 134 concentrations up to 30 wt%. Primary and secondary amines react with CO₂ to produce ammonium
 135 carbamates through the formation and deprotonation of zwitterion, as described in reactions 1 and
 136 2²⁵.



137 Tertiary amine reaction does not form zwitterion. Tertiary amines produce an unstable carbamate,
 138 and an additional reaction leads to the generation of bicarbonate ions (reaction 3). This reaction
 139 increases theoretical CO₂ loading compared to primary and secondary amines²⁶.



140 According to the literature, primary amines require more regeneration energy than tertiary
 141 amines²⁷. The reported value for MEA is 5 MJ/kg_{CO₂}, while MDEA presents values of 2.8
 142 MJ/kg_{CO₂} with stripper temperatures between 100 and 120 °C²⁸. A similar behaviour presents the
 143 CO₂ loading capacity with values close to 0,6 mol_{CO₂}/mol_{amine} for amine primaries²⁹ and 0.7
 144 mol_{CO₂}/mol_{amine} for tertiary amines³⁰. Despite this, primary and secondary amines are mainly used
 145 because carbamate formation exceeds those of bicarbonate. Several research works display that
 146 reaction constant can vary from 47740 m³/s/kmol for DETA³¹ to 8400 m³/s/kmol for MEA(32)
 147 and 11.15 m³/s/kmol for MDEA³⁰. Table 4 shows the average regeneration heat values and the
 148 main physical-chemical properties of the amines at a concentration of 30 wt%.

149 Table 4. Amine properties at 30wt% and 313 K.

Solvent	Rate constant reaction [m ³ /kmols]	Absorption heat [kJ/kmol _{CO₂}]	CO ₂ loading [mol _{CO₂} /mol _{amine}]	Reference
Ethanolamine (MEA)	8400	85.13	0.59	29,33
Diethanolamine (DEA)	1340	74.24	0.61	29,33,34
Triethylamine (TEA)	16.8	66.59	0.38	29,33,34
Piperazine (Pz)	53700	80.58	0.91	35,36
Aminomethyl propanol (AMP)	21000	80.91	0.78	29,33,34
Methyl diethanolamine (MDEA)	11.5	52.51	0.74	30,37
Diethylenetriamine (DETA)	47000	89.48	1.414	38, 39, 40

150 In the present research, a primary amine (MEA) and a tertiary amine (MDEA) have been selected
 151 to compare the maximum CO₂ capture rate (CCR). Capture rates are expected to depend on the
 152 variation of engine rotational speed and engine load conditions. The regeneration heat is obtained
 153 employing equation 1, which relates to the heat given up by the exhaust gases in the stripper (see
 154 Figure 1) and the CO₂ mass captured.

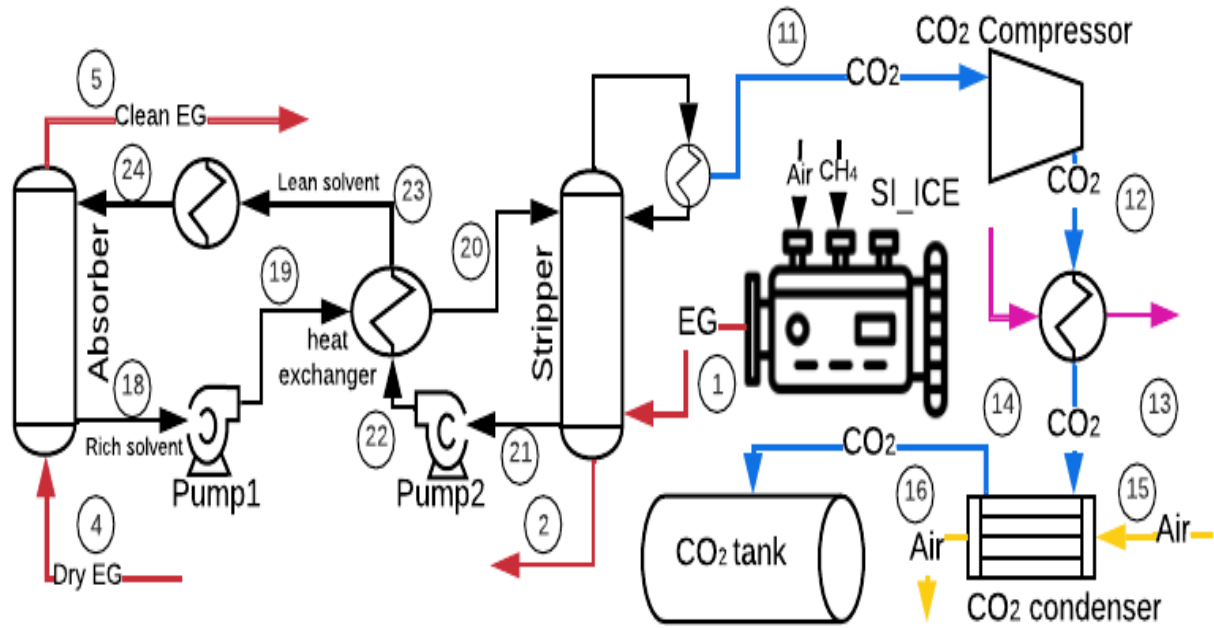
$$Q_{regeneration} = \frac{Q_{exhaust\ gases}}{m_{CO_2-storage}} \quad (1)$$

155 2.2.2. CCS configuration

156 According to the literature, amine scrubbing has a great potential to be used as a technique of CO₂
 157 capture onboard ICEv⁷: Figure 1 displays the amine scrubbing facility and the CO₂ compress
 158 process diagram. The exhaust gases from the ICE are used to heat the stripper and produce solvent
 159 regeneration (1). The desorption temperature is set to 120 °C to avoid corrosion problems and high
 160 solvent degradation. A pinch delta temperature of 10 °C is assumed, whereby the exhaust gases at
 161 the stripper outlet are fixed to be 130 °C (2). After releasing heat in the ORC, the exhaust gases
 162 are cooled down and dried to 40 °C before entering the bottom absorber (4). The lean solvent
 163 enters at the top of the column (24). The countercurrent flows of solvent and exhaust gases react
 164 in the absorber. The clean exhaust gas leaves the absorber at the top (5). Rich solvent leaves the
 165 column at the bottom (18), and it is pumped to the heat exchanger (19), where the temperature is
 166 raised to 87 °C before entering the top of the stripper (20). Lean solvent abandons at 101 °C and
 167 then goes to the heat exchanger and thus transfers thermal energy to the rich solvent (21-22),
 168 reducing its temperature to 84 °C. The lean solvent is cooled down until 40 °C in a cooler before
 169 entering again in the absorber. Finally, the water content in CO₂ flow is removed in the condenser,
 170 and high purity CO₂ gas flow goes to the compression stage (11). Table 5 summarised the
 171 parameters assumed in the simulations for the devices in the amine-scrubbing and CO₂
 172 compression facilities.

173 Table 5. Parameters of the amine-scrubbing and CO₂ compression devices assumed in the simulations

Device	Parameter	Value	Reference
Stripper	Operating temperature	120 °C	41
Absorber	Operating temperature	40 °C	42
Pumps 1 and 2	Isentropic efficiency	0.55	43
CO ₂ Compressor	Isentropic efficiency	0.65	43



174
175 Figure 1. Amine-scrubbing and CO₂ compression facilities diagram

176 2.2.3. CO₂ compression stage

177 The CO₂ is stored as a liquid to reduce its volume. To achieve this condition, the CO₂ will be
178 compressed from 1 bar to 75 bar (11-12) with two cooling stages until it reaches 29 °C. In the first
179 cooling stage, the CO₂ releases heat to the ORC (12-13), and in the second stage, the CO₂ is cooled
180 with atmospheric air under standard conditions (13-14). Finally, the CO₂ is stored in a tank, as
181 seen in Figure 1.

182 2.3. Organic cycle Rankine

183 2.3.1. Working fluid selection

184 Cyclopentane (C₅H₁₀) has been selected as a working fluid in the ORC. This working fluid (WF)
185 has had excellent results in previous ORC research on ICES⁴⁴. Also, it is thermally stable at
186 temperatures up to 350 °C⁴⁵. Another extensive factor for its selection is that C₅H₁₀ has a limited
187 environmental impact, low toxicity, and is non-corrosive⁴⁶.

188 2.3.2. ORC configuration

189 The configuration of the ORC was made following the procedure developed by Fatigati et al.^{43,47}.
190 This procedure calculates the maximum inlet pressure in the expander using equation 2.

$$P_{in,ex} = ZR(T_{sat} + \Delta T_{SH})\rho_{pmp,in}\beta_{\eta v}\beta_{Vol}\beta_{\omega} \quad (2)$$

191 This equation relates the inlet condition in the expander and pump of the ORC through
 192 dimensionless variables: $\beta_{\eta v}$ is the product of the volumetric efficiencies of the expander and
 193 pump; β_{Vol} is the ratio between the displacement volume of the pump and expander, and β_{ω} , is the
 194 ratio between the rotational speed of the pump and the expander. Maximum inlet pressure also
 195 depends on the superheating temperature difference (ΔT_{SH}) that increases with the engine load. The
 196 rest of the parameters in equation 1 are summarised in Table 6.

197 Table 6. Parameter values for the calculation of the inlet pressure to the expander

Variable	Value	Unit
compressibility factor (Z)	0.73	NA
R	0.1186	kJ/kg·K
T _{sat} at 25% of engine load (6.8 bar)	395.13	K
ΔT_{SH} at 25% engine load (6.8 bar)	0	K
ΔT_{SH} at 50% engine load (6.8 bar)	10	K
ΔT_{SH} at 75% engine load (6.8 bar)	23	K
ΔT_{SH} at 100% engine load (6.8 bar)	39	K
$\rho_{pump,in}$ at 1 bar (saturated liquid)	735,3	kg/m ³
$\eta_{vol,exp}$	0.45 ⁴⁸	NA
$\eta_{vol,pump}$	0.8 ⁴⁸	NA
$\beta_{\eta v}$	0.36	NA
β_{Vol}	0.5 ⁴⁸	NA
β_{ω}	0.2 ⁴⁸	NA

198 For a pump inlet pressure of 1 bar, the maximum pressure obtained at the expander inlet is 9.05
 199 bar. However, with the available heat in the exhaust gases after the stripper, the maximum
 200 saturation pressure achieved for the ORC cannot overcome 6.8 bar, whose value is less than the
 201 maximum allowed obtained with equation 2. So, the permeability value with 6.8 bar of expander
 202 inlet is 0.013 kg/MPa/s, which is a suitable permeability value according to the literature ⁴⁹.

203 With the values of low and high pressure found above, the ORC operation is under subcritical
 204 conditions. As there are two sources of heat (from the exhaust gases (2-3) and from the CO₂ after
 205 the compression process (12-13)), the ORC will have two evaporators (9-10-6). The pressure drop
 206 value in the evaporators is 1.1 bar for each one, which is taken from the literature⁴⁷. Finally, the
 207 ORC condenser cooling down the WF with air (7-8 and 16-17), whose pressure drop is 0,2 bar⁴⁷.
 208 This kind of ORC is called basic ORC (BORC)⁵⁰. Figure 2 displays the final configuration of the
 209 ORC, and Table 7 shows the values of the pressures and parameters considered for each device in
 210 the simulations.

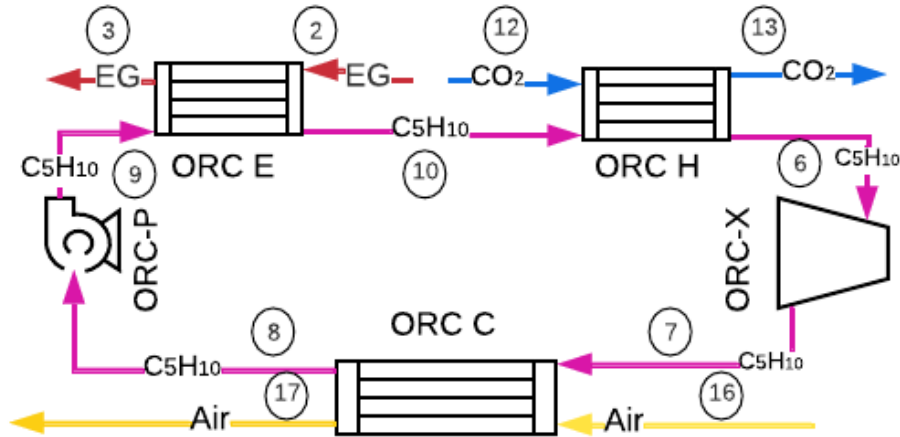


Figure 2. ORC layout used in the simulation

211
212

213 Table 7. Equipment conditions for ORC simulations

Equipment	Parameter	Unit	Value	State	Fluid
ORC-C	Inlet pressure	bar	1.2	Vapour	C ₅ H ₁₀
	Overall heat transfer coefficient ⁵¹	W/m ² K	500	Condensation	Air- C ₅ H ₁₀
ORC-P	Inlet pressure	bar	1	Saturated liquid	C ₅ H ₁₀
	Isentropic efficiency	NA	0.55	NA	
ORC-H	Inlet pressure	bar	9	Compressed liquid	C ₅ H ₁₀
	Overall heat transfer coefficient ⁵¹	W/m ² K	150	Liquid-Gas	C ₅ H ₁₀ - CO ₂
ORC-E	Inlet pressure	bar	7.9	Compressed liquid	C ₅ H ₁₀
	Overall heat transfer coefficient ⁵¹	W/m ² K	70 3000 35	Liquid-Gas Phase change Gas-Gas	C ₅ H ₁₀ - Exhaust gas
ORC-X	Inlet pressure	bar	6.8	Vapour	C ₅ H ₁₀
	Isentropic efficiency	NA	0.65	NA	

214 2.4. Simulation of the Hybridisation of the SI-ICE, CCS system and ORC

215 The amine scrubbing, CO₂ compression and ORC facilities were designed and modelled in Aspen
216 plus. These systems have been integrated to use the residual heat in the exhaust gases in the
217 desorption process and power production. Thus, to supply the power demand of the auxiliaries
218 such as pumps and compressors considered in the simulations.

219 Figure 3 shows the hybridisation of the four systems mentioned above. Additional parameters are
220 taken into account for the simulations: (i) concentration of the amine in the solvent is set to 30
221 wt%, (ii) mass fraction of the exhaust gases after the colling down process is 17.9% CO₂, 3% H₂O
222 and 79.1% N₂, and (iii) the full line pressure of the amine-scrubbing facility is maintained between
223 1 and 1.1 bar. Table 8 summarises all pressure and temperature values for each set point in the
224 simulations. Since these parameters are established in the simulations, it proceeds to obtain the

225 maximum CCR, the mass flow of solvent, WF, and cooling air, as well as the power and thermal
 226 energy consumption of each device.

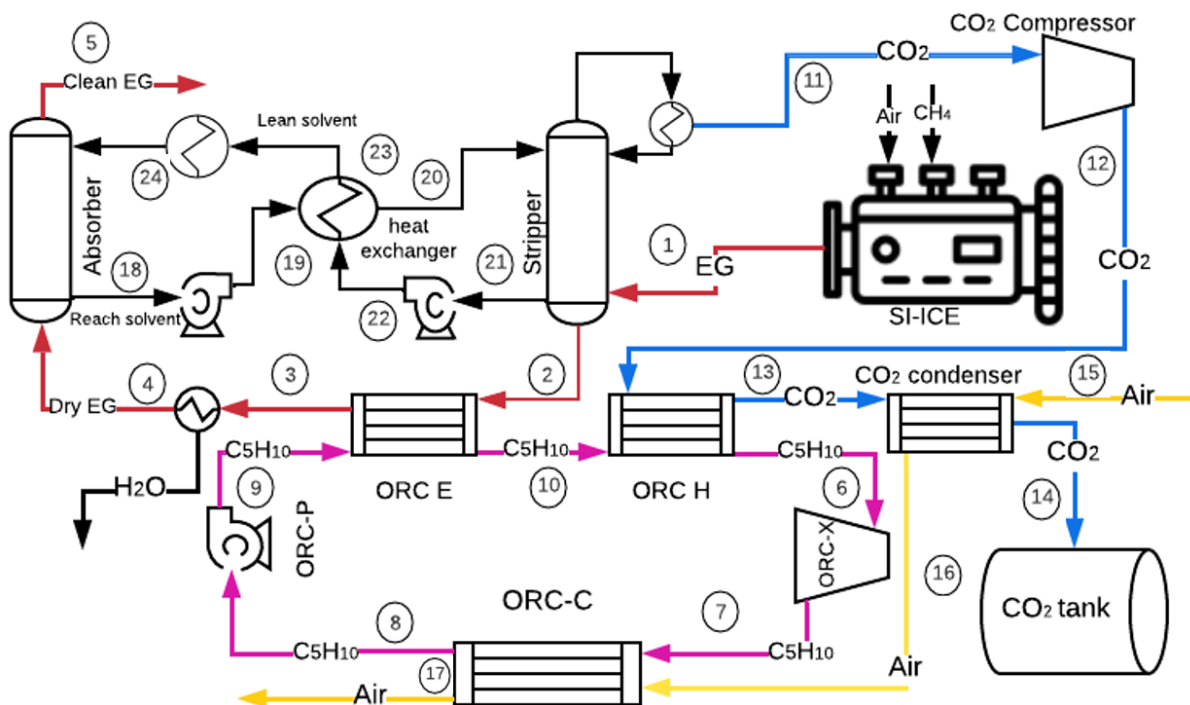


Figure 3. layout of the CCS system hybridised with the ORC

227
 228
 229

Table 8. Thermal conditions of the fluids in the simulations

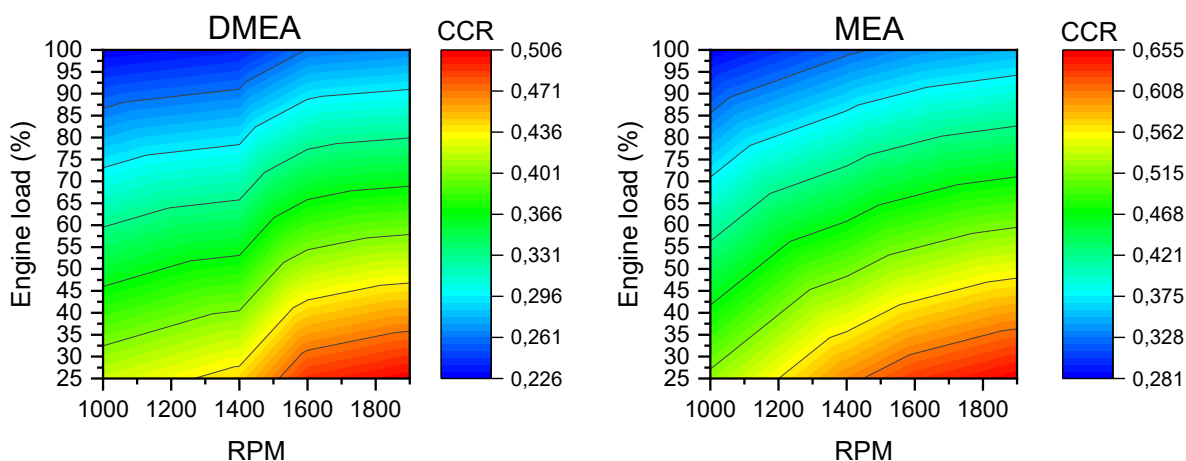
Point	Fluid	Quality	Pressure (bar)	Temperature (°C)
1, 2, 3	Exhaust gases (EG)	1	1.09	$f(\text{Engine load, rpm})$
4	EG	1	1.09	40
5	EG	1	1.09	$f(\text{absorber process})$
6	C ₅ H ₁₀	1	6,8	≥ 120
7	C ₅ H ₁₀	$f(\text{Engine load, rpm})$	1.2	$f(\text{C}_5\text{H}_{10} \text{ mass Flow})$
8	C ₅ H ₁₀	0	1	49
9	C ₅ H ₁₀	0	9	49
10	C ₅ H ₁₀	$f(\text{exhaust gases mass flow})$	7.9	122
11	CO ₂	1	1	40
12	CO ₂	1	75	565
13	CO ₂	1	75	≥ 120
14	CO ₂	0	75	29.3
15	Air	1	1	25
16	Air	1	1	$f(\text{CO}_2 \text{ mass flow})$
17	Air	1	1	$f(\text{C}_5\text{H}_{10} \text{ mass Flow})$
18	Rich solvent	1	1	$f(\text{absorber process})$
19	Rich solvent	1	1.1	$f(\text{absorber process})$
20	Rich solvent	1	1.1	87
21	Lean solvent	1	1	118
22, 23, 24	Lean solvent	1	1.1	$f(\text{stripper process})$

230
 231

3. Results

3.1. Amine capture

232 Figure 4 shows the CCRs obtained in the amine-scrubbing facility with the two amines selected at
 233 partial engine load in the entire rpm range. There, it can be observed that the highest CCRs occur
 234 at the lower engine load conditions and highest rpm, with values of 0.506 and 0.655 for MDEA
 235 and MEA, respectively. The lowest values of the CCRs are presented, at high engine load and
 236 lower rpm, with values of 0.226 for MDEA and 0.281 for MEA.

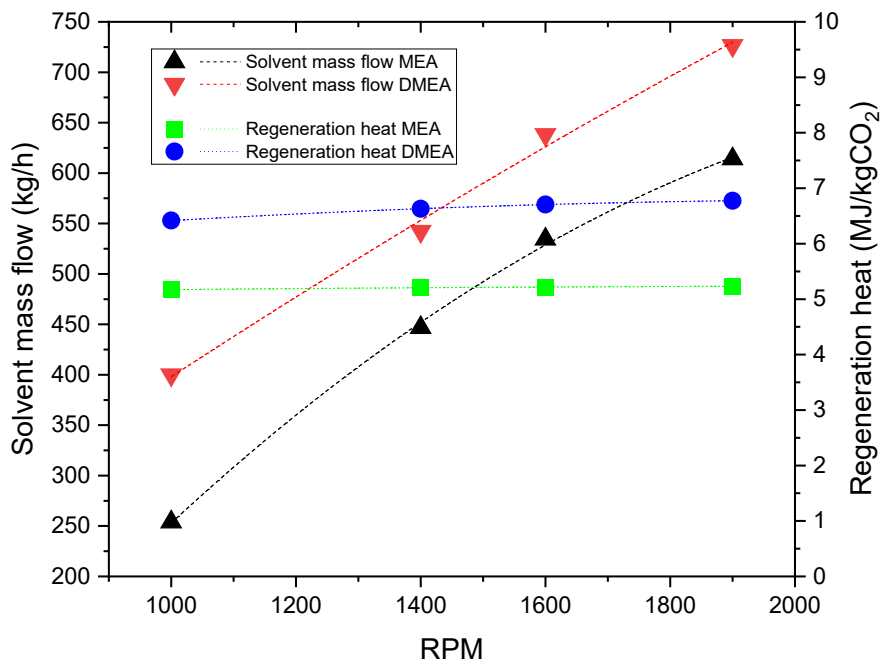


237
 238 Figure 4. CCRs for MEA and MDEA over the entire rpm range and at partial engine loads.

239 Comparing the two amines, the solvent with MEA captures 14.9% more than MDEA at its best
 240 operating condition (25% engine load and 1900 rpm) and 5.5% more at the worst working
 241 condition (100% engine load and 1000 rpm). The tendency with both amines is similar; they
 242 present a high CCR at low engine loads and higher rpm and a lower CCR at high engine loads and
 243 lower rpm. The reason is that the mass of CO₂ captured and the heat duty are the same for every
 244 engine load at a specific rotational speed (despite the increase in the exhaust gases' mass flow
 245 related to the engine load). These only increase with engine rotational speed and not with the
 246 engine load.

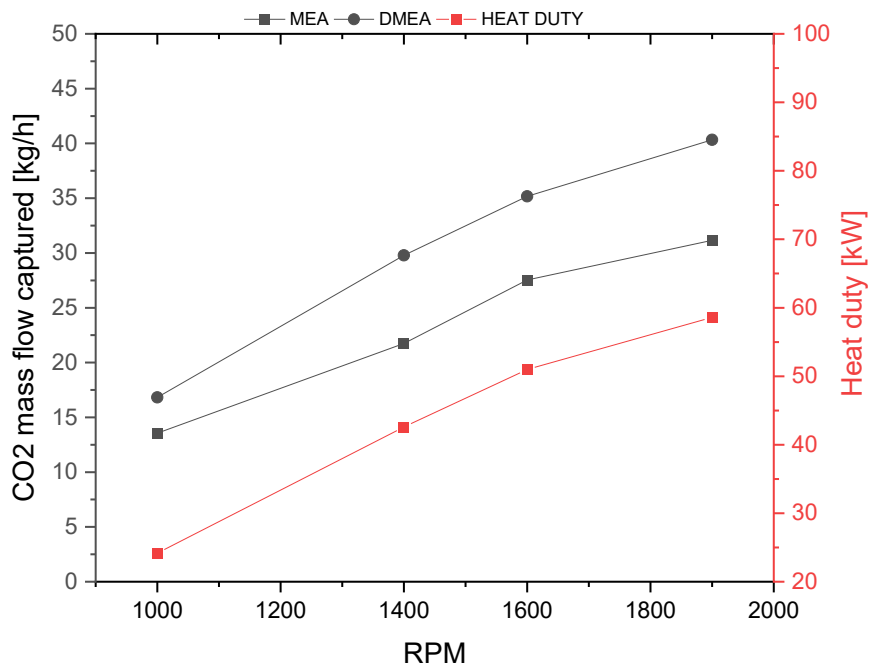
247 The heat duty for each rpm was always set up at 25 % of engine load with the aim that the stripper
 248 could operate in the other engine load conditions. For this reason, the heat duty in the stripper is
 249 kept constant for both amines. Thus, the reaction rate constant controls the CO₂ capture. MEA has
 250 a higher reaction rate coefficient than MDEA and can react with more CO₂ in the absorber
 251 resulting in a higher solvent mass flow and CCR than MDEA. Regeneration heat is directly
 252 affected, as a lower mass of CO₂ is captured for the same heat duty with MDEA, producing a
 253 regeneration heat 33% higher than with MEA in the entire rpm range. This behaviour is because

254 the CO₂ mass captured and the heat duty increase with the same slope. Figures 5 and 6 show the
 255 behaviours described above.



256
 257

Figure 5. Solvent mass flow and regeneration heat for loading conditions.



258
 259

Figure 6. Heat duty in stripper and CO₂ mass capturer with the amine selected

260 **3.2. ORC heat exchanger areas**

261 In order to be sure that the ORC can operate under all engine rpm and load conditions, the areas
 262 of the ORC and CO₂ compression system heat exchangers were obtained at the extreme points.
 263 Maximum engine load and 1900 rpm for the condensers and minimum load condition and 1000
 264 rpm for the areas of the evaporators were set. Table 9 shows the resulting areas in the simulations
 265 with each solvent.

266 Table 9. Heat exchangers areas obtained in the simulations

Amine	Heat exchanger	rpm	Engine load (%)	Exhaust gases mass flow (kg/h)	Area (m ²)	Variation (m ²)
MEA	Evaporator 1	1000	25	208,4	0.195	0.003
	Evaporator 2	1000	25	208,4	0.041	0.001
	ORC condenser	1900	100	754,7	0.361	0.0001
	CO ₂ condenser	1900	100	754,7	0.144	0.002
MDEA	Evaporator 1	1000	25	208,4	0.143	0.004
	Evaporator 2	1000	25	208,4	0.033	0.002
	ORC condenser	1900	100	754,7	0.284	0.001
	CO ₂ condenser	1900	100	754,7	0.109	0.003

267 As is shown in the previous results, the total heat exchanger area in the ORC is 0.741 m² with the
 268 MEA solution and 0.509 m² with MDEA. This difference is since there is less WF mass flow in
 269 the ORC with MDEA than MEA because there is less solvent in the amine-scrubbing facility. This
 270 situation produces less demand for cooling, whereby the CCS system operating with MDEA
 271 requires less air mass flow of cooling than with MEA. This behaviour can be seen in Figure 7.

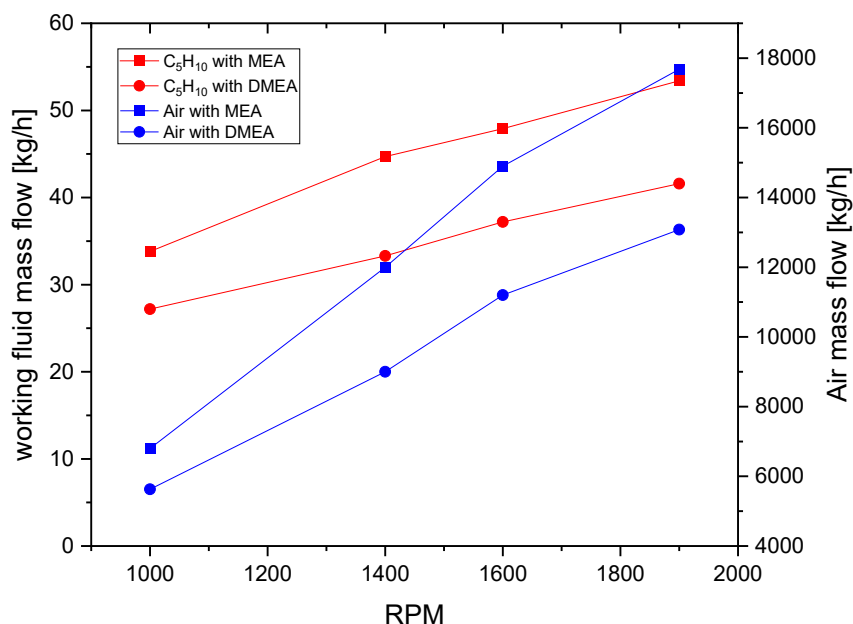
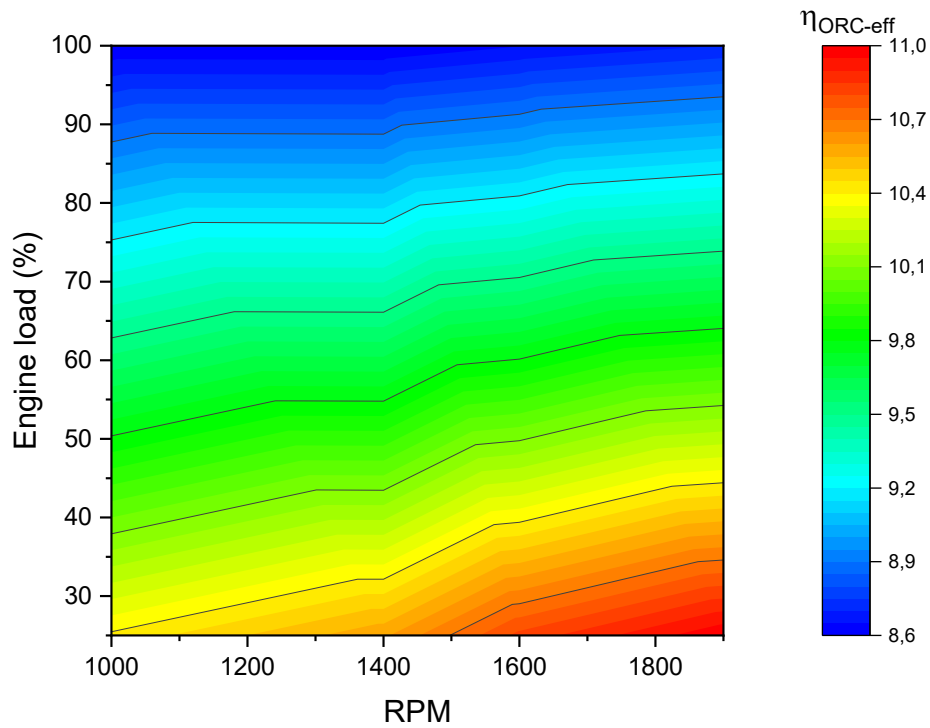


Figure 7. Working fluid and air mass flows in the ORC

272
 273

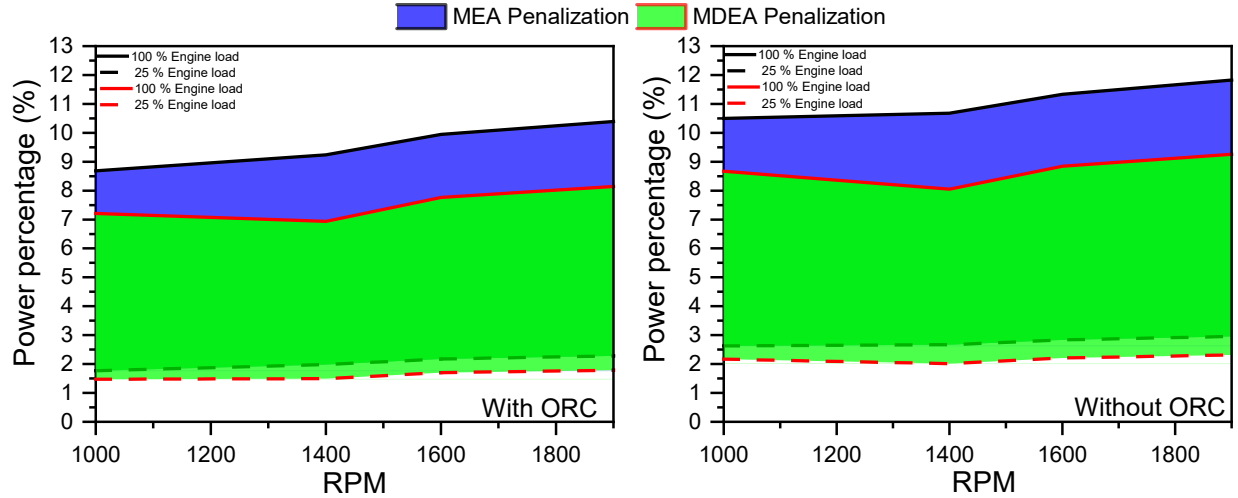
274 **3.3. Energy analysis**

275 The hybridisation of the ORC with the amine-scrubbing facility is done to further exploit the
276 thermal energy available in the exhaust gases after the solvent regeneration process. This
277 configuration tries to minimise the energy requirements of CO₂ storage, associated mainly with
278 CO₂ compression. Figure 8 shows that the ORC thermal efficiency reaches a maximum of 11% at
279 1900 rpm and 25% engine load and a minimum of 8.6% at 1000 rpm and full engine load. This
280 behaviour is the same with both solvents in the ORC, as it only depends on the available heat from
281 the exhaust gases after the stripper. Values agree with those reported in the literature for the
282 simulation of internal combustion engines operating with ORC ^{49,52,53,54}.



283
284

Figure 8. ORC efficiency over the entire engine rpm range and engine load conditions.



285
286 Figure 9. Percentage of power penalised of the engine by the CCS system with and without ORC.

287 The penalisation power percentage on the engine performance is calculated by adding the power
288 ORC expander, the CO₂ compression power and the powers of the ORC and CCS pumps and
289 dividing all this by the engine power (equation 3).

$$Power\ percentage = \frac{-\dot{W}_{ORC-X} + \dot{W}_{ORC-P} + \dot{W}_{Pump1} + \dot{W}_{Pump2} + \dot{W}_{CO_2-compressor}}{BP} \quad (3)$$

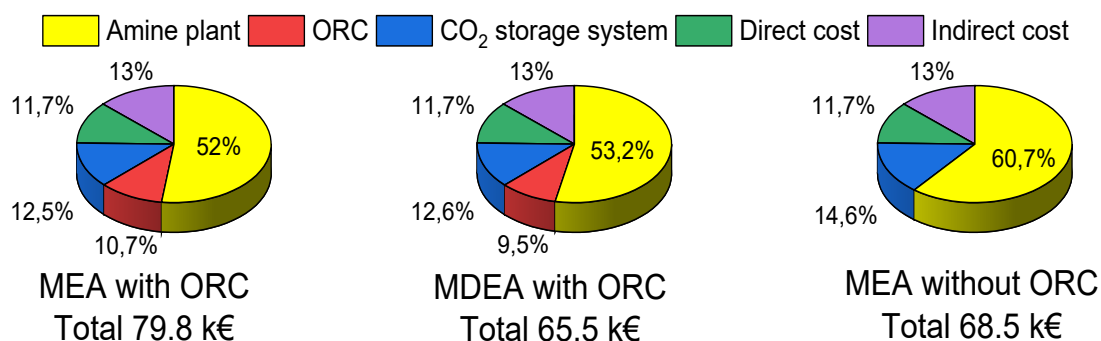
290 Figure 9 shows that the CCS system with MEA and working with the ORC has a penalisation on
291 the engine at its most critical point of 10.1%, while with MDEA, it is 8%. The difference is that
292 more CO₂ is captured with MEA, so more CO₂ compression power is required. However, the
293 simulations of the CCS system without ORC produce a penalisation on the engine power on
294 average 1.5% higher than the CCS system with ORC for both solvents. In contrast, at the lowest
295 point, the penalisation of the engine power is hardly noticeable.

296 3.4.Economic analysis

297 The economic analysis of the entire CCS is carried out with and without ORC for MEA and only
298 with ORC for MDEA. Devices costs are obtained through equations found in the literature. The
299 total capital investment (CAPEX) is completed after including the direct and indirect costs. Table
300 10 shows the equations used to calculate the CAPEX of the CCS system with the unit of waste
301 heat recovery. The result is added to the value of an NG-fuelled bus, and they are compared with
302 other commercial buses with CO₂ reduction technologies.

303 Table 90. CO₂ capture equipment installation costs CAPEX

Process	Equipment	Cost equation	Parameter (A)	Ref.
Amine plant	All equipment's	$26.094 \times 106(A/408)^{0.65}$	CO ₂ captured (t/h)	55,56
ORC	ORC-X	$1.5(225+170A)$	Volume (m ³)	58
	ORC-P	$900(A/300)^{0.25}$	Power (kW)	
	ORC-fan	$900(A/300)^{0.25}$	Power (kW)	
	ORC-C ₅ H ₁₀ tank	$31.5+16A$	Volume (L)	
	ORC-Evaporator	$190+310A$	Area (m ²)	
	ORC-H	$190+310A$	Area (m ²)	
	ORC-C	$190+310A$	Area (m ²)	
CO ₂ storage system	Condenser	$190+310A$	Area (m ²)	58
	Compressor	$267000(A/445)^{0.67}$	Power (kW)	59
	CO ₂ tank	$31.5+16A$	Volume (L)	58
Direct cost	Installing	8%A	Amineplant+ORC+CO ₂ storage system	Own criterion
	Instrumentation	5%A		
	Piping	1.5%A		
	Electric installing	1%A		
Indirect cost	Engineering	7%A	Amineplant+ORC+CO ₂ storage system+ direct cost	55
	Contingency	8%A		



304
305 Figure 10. Total CAPEX and percentage weight of each item included in the CAPEX

306 Figure 10 shows the percentage of the different items taken into account in the CAPEX and the
 307 total investment of the CCS system. It can be seen that amine plant cost has a weight greater than
 308 50% in the three cases, while the importance of the ORC cost over the total is between 9.5 and
 309 10.7%, depending on the amine used in the amine plant. As mentioned above, this is due to the
 310 size of the heat exchangers and compressor of CO₂.

311 The results show that with MEA, the CAPEX is 14.3 k€ higher than with MDEA. This difference
 312 is because the CCS system with MEA has a higher CCR than MDEA, requiring larger devices,
 313 which increases its cost. The CAPEX of the capture system without ORC using MEA is 14.1%
 314 lower regarding the base case. To conclude about the economic viability of a bus with a CCS
 315 system, a search of bus prices that using different CO₂ reduction technologies such as hydrogen
 316 fuel cell buss (HFCB) and electric battery (EB) bus has been done. Table 11 shows the bus prices
 317 found.

318 *Table 101. Purchase of passenger transport buses in euros*

Technology or fuel	Value (k€)	Difference from the base case (%)	Reference
CNG	374.6	0,0	60,61
Diesel	342.9	8,5	61
HFCB	650	-73,5	62
EB	604	-61,2	63
CNG+CCS+ORC	454.4	-21,3	Own study
CNG+CCS	443.1	-18,3	Own Study

319 According to the bus prices shown in Table 11, diesel bus is still the best alternative when it comes
 320 to the initial investment, as they are 8.5% cheaper than the base case. However, it is well known
 321 that high pollutant emissions, mainly particulate matter and nitrogen oxide emissions, are the
 322 Achilles heel of diesel buses. On the other hand, it is observed that the price of a bus with a CCS
 323 is about 40 percentage points below that of hydrogen fuel cell and battery-electric buses.

324 From the obtained data, installing a capture system increases the cost of the CNG-fuelled bus by
 325 18.3 to 21.3%. However, when the transport sector must pay for carbon Permits, the CCS in ICEv
 326 and the fuel cell system will be the best choice for the conventional vehicle. Based on the above,
 327 the fuel cell bus becomes more relevant because it does not emit CO₂. In the second place, it would
 328 be the vehicle with a capture system as it would achieve a CO₂ reduction of up to 66%, making it
 329 much more competitive than its conventional diesel counterpart. However, CCR is not enough to
 330 reach a totally CO₂-neutral system, unlike electric and hydrogen cell vehicles. Nevertheless, a bus
 331 with a CCS system with a 1 m³ storage tank at the conditions set out in this study could have
 332 autonomy up to 600 km (calculated with fuel consumption of 0.68 kg/km⁶⁴), which is 2.4 times
 333 longer than the current maximum range of commercial electric vehicles, which is 250 km on
 334 average⁶⁵.

335 **Conclusions**

336 A thermo-economic study of onboard CO₂ capture using amine scrubbing of a vehicle powered
 337 by a spark-ignition turbocharged internal combustion engine operating on natural gas has been
 338 carried out. According to the obtained results, the amine with the highest potential for CO₂ capture
 339 is MEA, having a higher CO₂ capture rate than MDEA under the whole range of engine operating
 340 conditions. However, the thermal integration of the exhaust gases with the CCS systems and ORC
 341 is technically feasible only for the CCS system. Because the exhaust gases can cover the desorption
 342 process of the CO₂ captured, but with the thermal energy reaming in the exhaust gases after the
 343 stripper, the ORC cannot produce enough power to reduce the penalisation on the performance

344 engine. Also, incorporating an ORC into the capture system does not offer a real benefit in terms
 345 of energy and economy. On the contrary, it would add weight and volume to the bus, increasing
 346 the vehicle's operating and maintenance costs.

347 The present study provides a first approximation to the use of amines in onboard capture. It would
 348 also be necessary to conduct detailed research on the reaction of amines with other pollutants in
 349 the exhaust gases, absorber and stripper sizing, and engine operation problems due to the resistance
 350 offered by the systems to the exhaust gases detrimental to engine performance.

351 Although this type of application in the transport sector is still in its initial research phase, the
 352 thermo-economic results obtained in this research show that a CCS by amine scrubbing with MEA
 353 and without ORC can become a competitive alternative to BEV and FCV, in particular in long
 354 distances. These capture-equipped vehicles will bring the transport sector closer to meeting the
 355 CO₂ reduction targets set by the European Union.

356 Nomenclature

Basic ORC	BORC	Internal combustion engine	ICE
Battery electric vehicles	BEV	Lower heating value	LHV
Brake power	BP	Methyldiethanolamine	MDEA
Brake-specific fuel consumption	BSFC	Monoethanolamine	MEA
Capital expenditure	CAPEX	Natural gas	NG
CO ₂ capture rates	CCR	Organic Rankine cycle	ORC
CO ₂ capture storage	CCS	Piperazine	PZ
Compressibility factor	Z	Saturation temperature	T _{sat}
Density	ρ	Ship-based carbon capture	SBCC
Exhaust gas recirculation	EGR	Spark ignition	SI
Fuel cell vehicles	FCV	Superheating temperature difference	ΔT _{SH}
ICE vehicles	ICEv	Temperature swing adsorption	TSA
Ideal gas constant	R	Waste energy recovery system	WERS

357 References

- 358 1. Kouridis C, Vlachokostas C. Towards decarbonising road transport: Environmental and social
 359 benefit of vehicle fleet electrification in urban areas of Greece. *Renewable and Sustainable Energy*
 360 *Reviews*. 2022 Jan 1;153:111775.
- 361 2. Auer M, Ganzer G, Müller-Baum P, Stiesch G. Synthetic Fuels in Large Engines - How Internal
 362 Combustion Engines Become CO₂-neutral. *MTZ worldwide*. 2019 Mar 8;80(3):48–51.
- 363 3. L'Orange Seigo S, Dohle S, Siegrist M. Public perception of carbon capture and storage (CCS): A
 364 review. *Renewable and Sustainable Energy Reviews*. 2014 Oct 1;38:848–63.
- 365 4. Rubin ES. Understanding the pitfalls of CCS cost estimates. *International Journal of Greenhouse*
 366 *Gas Control*. 2012 Sep 1;10:181–90.

- 367 5. García-Mariaca A, Llera-Sastresa E. Review on Carbon Capture in ICE Driven Transport. *Energies*
368 2021, Vol 14, Page 6865.
- 369 6. Leeson D, mac Dowell N, Shah N, Petit C, Fennell PS. A Techno-economic analysis and systematic
370 review of carbon capture and storage (CCS) applied to the iron and steel, cement, oil refining and
371 pulp and paper industries, as well as other high purity sources. *International Journal of Greenhouse*
372 *Gas Control*. 2017 Jun 1;61:71–84.
- 373 7. Sullivan JM, Sivak M. Carbon capture in vehicles: a review of general support, available
374 mechanisms, and consumer acceptance issues [Internet]. University of Michigan Transportation
375 Research Institute. 2012. Available from: <http://deepblue.lib.umich.edu/handle/2027.42/90951>
- 376 8. Schmauss TA, Barnett SA. Viability of Vehicles Utilising On-Board CO₂ Capture. Vol. 6, *ACS Energy*
377 *Letters*. American Chemical Society; 2021. p. 3180–4.
- 378 9. Awoyomi A, Patchigolla K, Anthony EJ. CO₂/SO₂ emission reduction in CO₂ shipping infrastructure.
379 *International Journal of Greenhouse Gas Control*. 2019;88:57–70.
- 380 10. Stec M, Tatarczuk A, Iluk T, Szul M. Reducing the energy efficiency design index for ships through
381 a post-combustion carbon capture process. *International Journal of Greenhouse Gas Control*.
382 2021;108(May 2020).
- 383 11. Güler E, Ergin S. An investigation on the solvent based carbon capture and storage system by
384 process modeling and comparisons with another carbon control methods for different ships.
385 *International Journal of Greenhouse Gas Control*. 2021 Sep 1;110:103438.
- 386 12. Ros JA, Skylogianni E, Doedée V, van den Akker JT, Vredeveldt AW, Linders MJG, et al.
387 Advancements in ship-based carbon capture technology on board of LNG-fuelled ships.
388 *International Journal of Greenhouse Gas Control*. 2022 Feb 1;114:103575.
- 389 13. Luo X, Wang M. Study of solvent-based carbon capture for cargo ships through process modelling
390 and simulation. *Applied Energy*. 2017;195:402–13.
- 391 14. Feenstra M, Monteiro J, van den Akker JT, Abu-Zahra MRM, Gilling E, Goetheer E. Ship-based
392 carbon capture onboard of diesel or LNG-fuelled ships. *International Journal of Greenhouse Gas*
393 *Control*. 2019;85(March):1–10.
- 394 15. Sharma S, Maréchal F. Carbon Dioxide Capture From Internal Combustion Engine Exhaust Using
395 Temperature Swing Adsorption. *Frontiers in Energy Research*. 2019;7(December):1–12.
- 396 16. Kumar P, Rathod V, Parwani AK. Experimental investigation on performance of absorbents for
397 carbon dioxide capture from diesel engine exhaust. *Environmental Progress & Sustainable Energy*.
398 2021 Apr 25;e13651.
- 399 17. Saravanan S, Kumar R. Experimental Investigations on CO₂ Recovery from Engine Exhaust Using
400 Adsorption Technology. *SAE Technical Paper*. 2019;2019-28–2577.
- 401 18. Osorio-Tejada JL, Llera-Sastresa E, Scarpellini S. Liquefied natural gas: Could it be a reliable option
402 for road freight transport in the EU? *Renewable and Sustainable Energy Reviews*.
403 2017;71(December 2015):785–95.


- 404 19. Mottschall M, Kasten P, Rodríguez F. Decarbonization of on-road freight transport and the role of
405 LNG from a German perspective. 2020;65.
- 406 20. Mercedes-Benz. Citaro NGT technical information [Internet]. 2017 [cited 2020 Feb 8]. p. 16.
407 Available from: [https://www.mercedes-benz-](https://www.mercedes-benz-bus.com/content/dam/mbo/markets/common/buy/services-online/download-technical-brochures/images/content/regular-service-buses/citaro-ngt/MB-NGT-2-ES-09_17.pdf)
408 [bus.com/content/dam/mbo/markets/common/buy/services-online/download-technical-](https://www.mercedes-benz-bus.com/content/dam/mbo/markets/common/buy/services-online/download-technical-brochures/images/content/regular-service-buses/citaro-ngt/MB-NGT-2-ES-09_17.pdf)
409 [brochures/images/content/regular-service-buses/citaro-ngt/MB-NGT-2-ES-09_17.pdf](https://www.mercedes-benz-bus.com/content/dam/mbo/markets/common/buy/services-online/download-technical-brochures/images/content/regular-service-buses/citaro-ngt/MB-NGT-2-ES-09_17.pdf)
- 410 21. Obiols J, Soleri D, Dioc N, Moreau M. Potential of concomitant injection of CNG and gasoline on a
411 1.6L gasoline direct injection turbocharged engine. SAE Technical Papers. 2011;
- 412 22. López JJ, Novella R, Gomez-Soriano J, Martinez-Hernandiz PJ, Rampanarivo F, Libert C, et al.
413 Advantages of the unscavenged pre-chamber ignition system in turbocharged natural gas engines
414 for automotive applications. Energy. 2021;218:119466.
- 415 23. Yontar AA, Doğu Y. Effects of equivalence ratio and CNG addition on engine performance and
416 emissions in a dual sequential ignition engine. International Journal of Engine Research.
417 2020;21(6):1067–82.
- 418 24. Wu Y, Xu J, Mumford K, Stevens GW, Fei W, Wang Y. Recent advances in carbon dioxide capture
419 and utilisation with amines and ionic liquids. Green Chemical Engineering. 2020 Sep 1;1(1):16–32.
- 420 25. Gouedard C, Picq D, Launay F, Carrette PL. Amine degradation in CO₂ capture. I. A review.
421 International Journal of Greenhouse Gas Control. 2012 Sep 1;10:244–70.
- 422 26. Chowdhury FA, Yamada H, Higashii T, Goto K, Onoda M. CO₂ capture by tertiary amine absorbents:
423 A performance comparison study. Industrial and Engineering Chemistry Research. 2013 Jun
424 19;52(24):8323–31.
- 425 27. Romeo LM, Minguell D, Shirmohammadi R, Andrés JM. Comparative Analysis of the Efficiency
426 Penalty in Power Plants of Different Amine-Based Solvents for CO₂ Capture. Industrial and
427 Engineering Chemistry Research. 2020 May 27;59(21):10082–92.
- 428 28. Cuccia L, Dugay J, Bontemps D, Louis-Louisy M, Vial J. Analytical methods for the monitoring of
429 post-combustion CO₂ capture process using amine solvents: A review. International Journal of
430 Greenhouse Gas Control. 2018 May 1;72:138–51.
- 431 29. Sada E, Hidehiro K, Butt MA. Gas Absorption with Consecutive Chemical Reaction: Absorption of
432 Carbon Dioxide into Aqueous Amine Solutions Chemical absorption mechanism. The Canadian
433 Journal of Chemical Engineering. 1976;54(5):421–4.
- 434 30. Ali BS, Aroua MK. Effect of piperazine on CO₂ loading in aqueous solutions of MDEA at low
435 pressure. International Journal of Thermophysics. 2004;25(6):1863–70.
- 436 31. Hartono A, da Silva EF, Svendsen HF. Kinetics of carbon dioxide absorption in aqueous solution of
437 diethylenetriamine (DETA). Chemical Engineering Science. 2009 Jul 15;64(14):3205–13.
- 438 32. Hikita H, Asai S, Katsu Y, Ikuno S. Absorption of carbon dioxide into aqueous monoethanolamine
439 solutions. AIChE Journal. 1979 Sep;25(5):793–800.

- 440 33. el Hadri N, Quang DV, Goetheer ELV, Abu Zahra MRM. Aqueous amine solution characterisation
441 for post-combustion CO₂ capture process. *Applied Energy*. 2017 Jan 1;185:1433–49.
- 442 34. Kim YE, Lim JA, Jeong SK, Yoon Y il, Bae ST, Nam SC. Comparison of carbon dioxide absorption in
443 aqueous MEA, DEA, TEA, and AMP solutions. *Bull Korean Chem Soc*. 2013;34(3):783–7.
- 444 35. Chen X, Rochelle GT. Aqueous piperazine derivatives for CO₂ capture: Accurate screening by a
445 wetted wall column. *Chemical Engineering Research and Design*. 2011;89(9):1693–710.
- 446 36. Bishnoi S, Rochelle GT. Absorption of carbon dioxide into aqueous piperazine: Reaction kinetics,
447 mass transfer and solubility. *Chemical Engineering Science*. 2000;55(22):5531–43.
- 448 37. Wang Y, Zhao L, Otto A, Robinius M, Stolten D. A Review of Post-combustion CO₂ Capture
449 Technologies from Coal-fired Power Plants. *Energy Procedia*. 2017;114(November 2016):650–65.
- 450 38. Derks PWJ, Versteeg GF. Kinetics of absorption of carbon dioxide in aqueous ammonia solutions.
451 *Energy Procedia*. 2009;1(1):1139–46.
- 452 39. Fu K, Sema T, Liang Z, Liu H, Na Y, Shi H, et al. Investigation of mass-transfer performance for CO₂
453 absorption into diethylenetriamine (DETA) in a randomly packed column. *Industrial and
454 Engineering Chemistry Research*. 2012;51(37):12058–64.
- 455 40. Kim YE, Moon SJ, Yoon Y Il, Jeong SK, Park KT, Bae ST, et al. Heat of absorption and absorption
456 capacity of CO₂ in aqueous solutions of amine containing multiple amino groups. *Separation and
457 Purification Technology*. 2014;122:112–8.
- 458 41. Nakagaki T, Yamabe R, Furukawa Y, Sato H, Yamanaka Y. Experimental Evaluation of Temperature
459 and Concentration Effects on Heat of Dissociation of CO₂-loaded MEA Solution in Strippers. *Energy
460 Procedia*. 2017 Jul 1;114:1910–8.
- 461 42. Søndery TL, Carlsen KB, Fosbøl PL, Kjørboe LG, von Solms N. A new pilot absorber for CO₂ capture
462 from flue gases: Measuring and modelling capture with MEA solution. *International Journal of
463 Greenhouse Gas Control*. 2013 Jan 1;12:181–92.
- 464 43. Fatigati F, di Battista D, Cipollone R. Permeability effects assessment on recovery performances of
465 small-scale ORC plant. *Applied Thermal Engineering*. 2021 Sep 1;196:117331.
- 466 44. Invernizzi CM, Iora P, Manzolini G, Lasala S. Thermal stability of n-pentane, cyclo-pentane and
467 toluene as working fluids in organic Rankine engines. *Applied Thermal Engineering*. 2017;121:172–
468 9.
- 469 45. Invernizzi CM, Bonalumi D. Thermal stability of organic fluids for Organic Rankine Cycle systems.
470 *Organic Rankine Cycle (ORC) Power Systems: Technologies and Applications*. Elsevier Ltd; 2017.
471 121–151 p.
- 472 46. Scaccabarozzi R, Tavano M, Invernizzi CM. Comparison of working fluids and cycle optimisation for
473 heat recovery ORCs from large internal combustion engines. *Energy*. 2018; 158, 396-416
- 474 47. Fatigati F, di Bartolomeo M, di Battista D, Cipollone R. Experimental and Numerical
475 Characterization of the Sliding Rotary Vane Expander Intake Pressure in Order to Develop a Novel
476 Control-Diagnostic Procedure. *Energies (Basel)*. 2019 May 23;12(10):1970.


- 477 48. Fatigati F, di Battista D, Cipollone R. Permeability effects assessment on recovery performances of
478 small-scale ORC plant. *Applied Thermal Engineering*. 2021 Sep 1;196:117331.
- 479 49. Fatigati F, di Bartolomeo M, di Battista D, Cipollone R. Experimental characterisation of a hermetic
480 scroll expander operating in an ORC-based power unit bottoming an internal combustion engine.
481 In: *AIP Conference Proceedings*. American Institute of Physics Inc.; 2019.
- 482 50. Peris B, Navarro-Esbrí J, Molés F. Bottoming organic Rankine cycle configurations to increase
483 Internal Combustion Engines power output from cooling water waste heat recovery. *Applied*
484 *Thermal Engineering*. 2013;61(2):364–71.
- 485 51. Matthias Kind and Holger Martin. *VDI Heat Atlas*. Second. Berlin: Springer ; 2010. 1–1609 p.
- 486 52. Badescu V, Aboaltabooq MHK, Pop H, Apostol V, Prisecaru M, Prisecaru T. Design and operational
487 procedures for ORC-based systems coupled with internal combustion engines driving electrical
488 generators at full and partial load. *Energy Conversion and Management*. 2017;139:206–21.
- 489 53. Shu G, Zhao M, Tian H, Wei H, Liang X, Huo Y, et al. Experimental investigation on thermal OS/ORC
490 (Oil Storage/Organic Rankine Cycle) system for waste heat recovery from diesel engine. *Energy*.
491 2016 Jul 15;107:693–706.
- 492 54. Hoang AT. Waste heat recovery from diesel engines based on Organic Rankine Cycle. *Applied*
493 *Energy*. 2018;231(March):138–66.
- 494 55. Abu-Zahra MRM, Niederer JPM, Feron PHM, Versteeg GF. CO₂ capture from power plants. Part II.
495 A parametric study of the economical performance based on mono-ethanolamine. *International*
496 *Journal of Greenhouse Gas Control*. 2007;1(2):135–42.
- 497 56. Bailera M, Espatolero S, Lisbona P, Romeo LM. Power to gas-electrochemical industry hybrid
498 systems: A case study. *Applied Energy*. 2017;202:435–46.
- 499 57. Astolfi M. Techno-economic Optimization of Low Temperature CSP Systems Based on ORC with
500 Screw Expanders. In: *Energy Procedia*. Elsevier Ltd; 2015. p. 1100–12.
- 501 58. Quoilin S, Declaye S, Tchanche BF, Lemort V. Thermo-economic optimisation of waste heat
502 recovery Organic Rankine Cycles. *Applied Thermal Engineering*. 2011;31(14–15):2885–93.
- 503 59. De Saint Jean M, Baurens P, Bouallou C, Couturier K. Economic assessment of a power-to-
504 substitute-natural-gas process including high-temperature steam electrolysis. *International*
505 *Journal of Hydrogen Energy*. 2015 Jun 1;40(20):6487–500.
- 506 60. Ally J, Pryor T. Life cycle costing of diesel, natural gas, hybrid and hydrogen fuel cell bus systems:
507 An Australian case study. *Energy Policy*. 2016 Jul 1;94:285–94.
- 508 61. Holland SP, Mansur ET, Muller NZ, Yates AJ. The environmental benefits of transportation
509 electrification: Urban buses. *Energy Policy*. 2021 Jan 1;148.
- 510 62. Spendelow J, Papageorgopoulos D, Satyapal S. *Fuel Cell Technologies Program Record 12012: Fuel*
511 *Cell Bus Targets*. 2012.

- 512 63. Quarles N, Kockelman KM, Mohamed M. Costs and Benefits of Electrifying and Automating Bus
513 Transit Fleets. Sustainability. 2020 May 13;12(10):3977.
- 514 64. Stempien JP, Chan SH. Comparative study of fuel cell, battery and hybrid buses for renewable
515 energy constrained areas. Journal of Power Sources. 2017 Feb 1;340:347–55.
- 516 65. Wenz KP, Serrano-Guerrero X, Barragán-Escandón A, González LG, Clairand JM. Route prioritisation
517 of urban public transportation from conventional to electric buses: A new methodology and a
518 study of case in an intermediate city of Ecuador. Renewable and Sustainable Energy Reviews. 2021
519 Sep 1;148:111215.

520

	<p>Alexander García-Mariaca is a male PhD candidate at Zaragoza University in renewable energy and energy efficiency. Alex's research focuses on the CO₂ capture process in mobile sources. He also has researched in performance and emissions of internal combustion engines, fluids dynamics, heat transfer, turbomachinery, and mathematical modelling.</p>
---	--

521

	<p>Eva Llera is an Associate Professor in the Thermal Machines and Engines Area at the University of Zaragoza (Spain). Her research experience covers 20 years and has focused on two parallel research lines: energy socioeconomics and energy sustainability in activity sectors.</p>
---	---

522